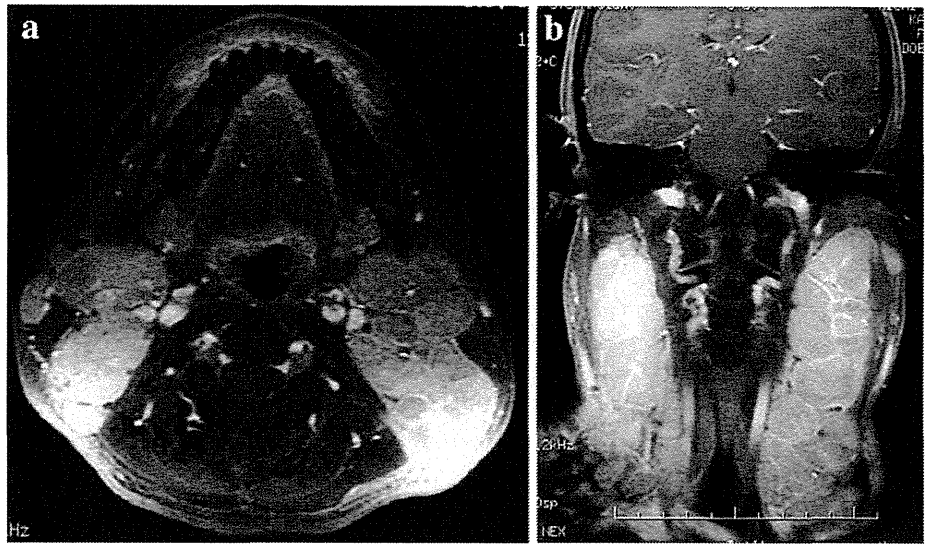

Fig. 2 Contrast-enhanced MRI of the neck. Lymphadenopathy in both sides of the neck on an axial section (**a**) and a coronal section (**b**)

Prophylactic nodal irradiation was not used. Planning target volume (PTV) was defined as CTV with 5-mm margins in all dimensions. Normal structures such as organs at risk (OAR) included the brainstem, spinal cord, brain, lens, eyeball, optic chiasma, optic nerve, inner ear, oral cavity, mandible, parotid gland, larynx, and lung. A planning dose at D95 (95% of the PTV receiving the prescribed dose) was prescribed to the PTV at 50 Gy in 25 fractions. Other radiotherapy-planning techniques and the dose constraints for OAR were similar to those in a report on nasopharyngeal cancer [8]. The patient received daily MVCT acquisitions for setup verification. Figure 3 shows a dose–volume histogram (DVH) and dose distributions of the patient. At the midcourse of radiation treatment, another kilovolt CT was taken to evaluate the change of dose distribution caused by shrinkage of tumor or body weight loss. A CT scan for evaluation for change of dose distribution was archived in the Tomoprovider and an adaptive dose distribution was made from these images using the initial planning beam data on the DQA system. The adaptive dose distribution was evaluated visually using the dose coverage of PTV and the change of dose distribution on the cord, stem, and parotid gland. Because the dose distribution of PTV and these OAR seemed acceptable, we did not change the RT plan. This patient experienced some acute toxicity including grade 3 mucositis, grade 2 dysgeusia, grade 2 xerostomia, and a grade 2 skin reaction on the National Cancer Institute's (NCI) Common Toxicity Criteria, version 3.0. The patient required temporary interruption of IMRT because of this acute toxicity. Finally, the total dose was reduced to 44 Gy in 22 fractions over 46 days. The cervical lymphadenopathy shrank gradually during IMRT on physical examination (Fig. 4a, b), and the patient's discomfort due to cervical lymphadenopathy was relieved. At present, 4 years and 3 months after IMRT, no signs of tumor regrowth have been detected (Fig. 4c).

Parotid function was evaluated by quantitative salivary scintigraphy and the xerostomia grade using NCI toxicity criteria, version 3.0. Parotid saliva excretion was measured by the maximum excretion ratio (MER) in the parotid region on salivary scintigraphy. The method of salivary scintigraphy was similar to that in a report on nasopharyngeal cancer [8]. The MERs of the right salivary gland were 61.7, 25.1, and 48.7%, and those of the left salivary gland were 45.3, 19.0, and 35.9% before initial treatment, 3, and 12 months after the completion of IMRT, respectively. The parotid function of both sides was improved dramatically between 3 and 12 months after IMRT. Xerostomia was also improved from grade 2 to grade 0 between 3 and 12 months after IMRT.

Discussion

We report a case of cervical multicentric Castleman disease treated with IMRT using HT. Cervical lymphadenopathy shrank gradually during IMRT. Four years and 3 months after IMRT, no signs of regrowth of cervical lymphadenopathy have been detected. A standard approach to clinical management has yet to be agreed for multicentric Castleman disease. Primary RT has been described in numerous case reports and small case series as one strategy for treatment of both the unicentric and multicentric forms of Castleman disease. Vries et al. [5] presented an overview of all studies that evaluated the use of primary RT in

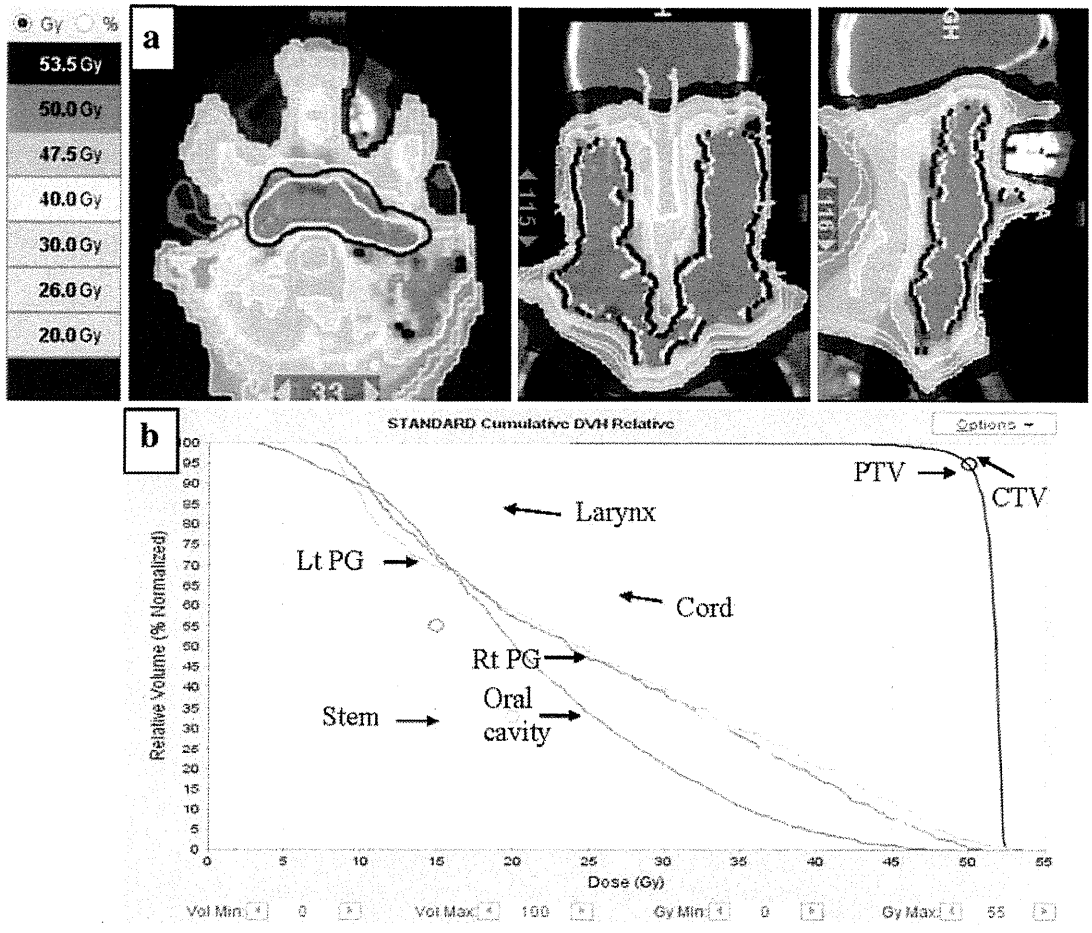

Fig. 3 Dose distribution for the patient with cervical multicentric Castleman disease. **a** Dose volume histogram (DVH) of typical normal structures as organ at risk (OAR) and target volume (**b**). *CTV* clinical target volume, *PTV* planning treatment volume, *PG* parotid gland, *IE* inner ear

Castleman disease, for both unicentric and multicentric disease, with doses ranging from 12 to 50 Gy. Responses to primary RT for treatment of both forms of Castleman disease ranged from no response to complete response. With regard to the dose of RT, no correlation could be observed between dose and response. Most patients were treated with a dose between 40 and 50 Gy; however, the dose of RT varied from 12 to 50 Gy in patients with a complete response. Other concerns about the RT method, for example an appropriate margin of GTV or the need for prophylactic irradiation, are issues for the future, because no study has evaluated correlation between RT methods and tumor control. Adaptive radiotherapy is an approach to correct for morphological changes in a patient's anatomy, for example tumor and normal tissue variations as a result of treatment [9]. We did not change the RT plan because the change of the dose distribution seemed acceptable.

As there is currently no consensus on treatment of multicentric Castleman disease, physicians tend to reject RT because of its toxicity, especially for head and neck lesions. In this case, the parotid function and xerostomia improved dramatically after IMRT. IMRT is an effective method to minimize xerostomia in head and neck lesions. There is also a little concern about radiation-induced second primary cancer or late complications, for example carotid artery stenosis in the long-term future. The clinical management of multicentric Castleman disease remains controversial, and we should recognize there are approaches other than RT, for example rituximab-based treatment or chemotherapy [10].

In conclusion, we report a case of cervical multicentric Castleman disease treated with IMRT using HT. To date, no signs of regrowth of cervical lymphadenopathy have been detected. The parotid function on quantitative salivary scintigraphy and xerostomia improved dramatically within

Fig. 4 Before IMRT. Lymphadenopathy in both sides of the neck. **a** At the time of completion of IMRT. Lymphadenopathy in both sides of the neck shrank. **b** Four years and 3 months after IMRT. No regrowth of lymphadenopathy was observed (**c**). *IMRT* intensity-modulated radiation therapy

12 months after completion of IMRT. RT could be an option for multicentric Castleman disease, and IMRT can reduce xerostomia compared with conventional RT in head and neck lesions.

Conflict of interest The authors declare no conflict of interest.

References

1. Castleman B, Towne VW. Case records of the Massachusetts General Hospital; weekly clinicopathological exercises; founded by Richard C. Cabot. N Engl J Med. 1954;251:396–400.
2. Keller AR, Hochholzer L, Castleman B. Hyaline-vascular and plasma-cell types of giant lymph node hyperplasia of the mediastinum and other locations. Cancer. 1972;29:670–83.
3. McCarty MJ, Vukelja SJ, Banks PM, Weiss RB. Angiofollicular lymph node hyperplasia (Castleman's disease). Cancer Treat Rev. 1995;21:291–310.
4. Dispenzieri A, Gertz MA. Treatment of Castleman's disease. Curr Treat Options Oncol. 2005;6:255–66.
5. de Vries IA, van Acht MM, Demeyere TB, Lybeert ML, de Zoete JP, Nieuwenhuijzen GA. Neoadjuvant radiotherapy of primary irresectable unicentric Castleman's disease: a case report and review of the literature. Radiat Oncol. 2010;5:7.
6. Moiseenko V, Wu J, Hovan A, Saleh Z, Apte A, Deasy JO, et al. Treatment planning constraints to avoid xerostomia in head-and-neck radiotherapy: an independent test of QUANTEC criteria using a prospectively collected dataset. Int J Radiat Oncol Biol Phys (in press).
7. Teh BS, Woo SY, Butler EB. Intensity modulated radiation therapy (IMRT): a new promising technology in radiation oncology. Oncologist. 1999;4:433–42.
8. Kodaira T, Tomita N, Tachibana H, Nakamura T, Nakahara R, Inokuchi H, et al. Aichi cancer center initial experience of intensity modulated radiation therapy for nasopharyngeal cancer using helical tomotherapy. Int J Radiat Oncol Biol Phys. 2009;73:1129–34.
9. Schwartz DL, Garden AS, Thomas J, Chen Y, Zhang Y, Lewin J, et al. Adaptive radiotherapy for head-and-neck cancer: initial clinical outcomes from a prospective trial. Int J Radiat Oncol Biol Phys (in press).
10. Bower M, Newsom-Davis T, Naresh K, Merchant S, Lee B, Gazzard B, et al. Clinical features and outcome in HIV-associated multicentric Castleman's disease. J Clin Oncol. 2011;29:2481–6.

J. Radiat. Res., 53, 138–144 (2012)

Evaluation of Parotid Gland Function using Equivalent Cross-relaxation Rate Imaging Applied Magnetization Transfer Effect

Hidetoshi SHIMIZU[1]*, Shigeru MATSUSHIMA[2], Yasutomi KINOSADA[3], Hiroki MIYAMURA[2], Natsuo TOMITA[1], Takashi KUBOTA[1], Hikaru OSAKI[1], Masashi NAKAYAMA[1], Manabu YOSHIMOTO[1] and Takeshi KODAIRA[1]

Radiotherapy/Function/ECRI/Scintigraphy/Parotid gland.

Safe imaging modalities are needed for evaluating parotid gland function. The aim of this study was to validate the utility of a magnetic resonance imaging (MRI) tool, equivalent cross-relaxation rate imaging (ECRI), as a measurement of parotid gland function after chemoradiotherapy. Subjects comprised 18 patients with head-neck cancer who underwent ECRI and salivary gland scintigraphy. First, we calculated ECR values (signal intensity on ECRI), maximum uptake rate (MUR) and washout rate (WOR) from salivary gland scintigraphy data at the parotid glands. Second, we investigated correlations between ECR values and each parameter of MUR (uptake function) and WOR (secretory function) obtained by salivary gland scintigraphy at the parotid gland. Next, we investigated each dose-response for ECR, MUR and WOR at the parotid gland. A correlation was detected between ECR values and MUR in both the pre- ($r = -0.55$, $p < 0.01$) and post-treatment ($r = -0.50$, $p < 0.05$) groups. A significant post-treatment correlation was detected between the percentage change in ECR values at 3–5 months after chemoradiotherapy and median dose to the parotid gland (Pearson correlation, $r = -0.62$, $p < 0.05$). However, no correlations were detected between median dose to the parotid gland and either MUR or WOR. ECRI is a new imaging tool for evaluating the uptake function of the parotid gland after chemoradiotherapy.

INTRODUCTION

Radiotherapy for head and neck cancers must be performed with care, as various high-risk organs are situated in the surrounding area. Decreasing side effects in these organs is thus problematic. The parotid gland shows high radiosensitivity and inclusion within the irradiation field during radiotherapy for head and neck cancer causes depression of parotid gland function. Evaluation of parotid gland function after radiotherapy has been performed using salivary gland scintigraphy.[1–3] This modality can evaluate parotid gland function by observing the movement of radionuclide ($^{99m}TcO_4^-$) that accumulates in the parotid gland. However, the use of radionuclides obviously means that radiation exposure for human bodies is unavoidable,[4] making this technique unsuitable for regular evaluation of parotid gland depression caused by radiotherapy.

Magnetic resonance imaging (MRI) uses magnetism and electromagnetic waves, representing a noninvasive modality with no exposure to radiation. The apparent diffusion coefficient (ADC) obtained by diffusion-weighted imaging has been reported as a parameter for evaluating parotid function.[5–7] However, ADC shows a low correlation coefficient with the function parameter obtained by salivary gland scintigraphy.[7]

We selected equivalent cross-relaxation rate imaging (ECRI) applied magnetization transfer effect using MRI.[8–12] ECRI can detect minute changes in organization and molecular structure, offering information reflecting interactions with water molecules and biomacromolecules.[8]

The aim of the present study was to validate the utility of ECRI for evaluating parotid gland function after chemoradiotherapy. ECRI provides difference information for parts irradiated with a single saturation pulse. ECRI can obtain cell-density-weighted images and fiber-density-weighted images by irradiating a saturation pulse close to or far from the center frequency of water, respectively.[10,12] The acinar

*Corresponding author: Phone: +81-52-762-6111.
Fax: +81-52-752-8390.
E-mail: hishimizu@aichi-co.jp
[1]Department of Therapeutic Radiation Oncology, Aichi Cancer Center Hospital, 1-1 Kanokoden, Chikusa-ku, Nagoya 464-8681, Japan; [2]Department of Diagnostic and Interventional Radiology, Aichi Cancer Center Hospital, 1-1 Kanokoden, Chikusa-ku, Nagoya 464-8681, Japan; [3]Department of Biomedical Informatics, Gifu University Graduate School of Medicine, 1-1 Yanagido, Gifu 501-1193, Japan.
doi:10.1269/jrr.11059

cell composing the parotid gland plays a big role to the uptake of saliva. Therefore, we irradiated with a saturation pulse at 7 ppm downfield from the center frequency of water to obtain cell-density-weighted images in this research. We first investigated correlations between ECR values (signal intensity on ECRI) at the parotid gland and parameters (uptake function and secretory function) as obtained by salivary gland scintigraphy. We then investigated each dose-response for ECR and salivary gland scintigraphy parameters in the parotid gland.

MATERIALS AND METHODS

Patients

Subjects comprised 18 patients with head and neck cancer. Table 1 shows patient characteristics. Disease was staged according to the American Joint Committee on Cancer 1997 clinical staging.[13] All patients received an explanation about the purpose and methods of this research and issues related to the protection of privacy, and informed consent to participate in the study was obtained prior to enrolment. MRI and salivary gland scintigraphy were performed in 6 patients before chemoradiotherapy, 6 patients after chemoradiotherapy and 6 patients both before and after chemoradiotherapy. As a result, 24 series of data were obtained for 48 parotid glands.

Chemoradiotherapy

All patients were immobilized in a cast, and computed tomography (CT) with 2.5 mm slice thickness was taken for treatment planning. Scans included the target area, regional lymph nodes, and the parotid glands. Target objects and normal structures including both parotid glands were contoured on a Pinnacle workstation (Hitachi Medical Corporation, Tokyo, Japan). Computed tomography (CT) images with the contour objects were transferred to a specific treatment planning system (Tomoprovider; TomoTherapy, Madison, WI).

Table 1. Patient characteristics

N	18
Male/female	15/3
Median age (range)	53 (16–74)
Tumor site	
Nasopharynx	16
Oropharynx	2
Stage	
I	1 (6%)
II	2 (11%)
III	8 (44%)
IV	7 (39%)

A dose of 66–70 Gy was prescribed to the primary tumor. Most patients were treated using a fractionation scheme with 2 Gy administered 5 times/week. One patient received 1.8 Gy per fraction. Dose constraints for parotid glands were mean dose < 30 Gy, median < 23 Gy and whole parotid gland volume with < 20 Gy > 20 mm^3. Other planning parameters comprised: primary collimator width, 2.5 cm; pitch, 0.3; and modulation factor, 3.0–4.0.

Radiotherapy was performed using a Hi-ART System (TomoTherapy), which is specifically designed for intensity-modulated radiotherapy (IMRT). All patients received daily megavoltage CT (MVCT) acquisitions for setup verification.[14,15]

Chemotherapy was planned for 16 patients, with only 2 patient undergoing radiotherapy alone, as medical condition was considered insufficient for systemic chemotherapy. Three courses of chemotherapy comprising continuous intravenous administration of 5-fluorouracil at 800 mg/m^2/24 h for 5 days (Days 1–5) and nedaplatin (NDP) at 130 mg/m^2/6 h for 1 day (Day 6) were administered approximately every 4 weeks in the alternating setting. The details of contents of chemoradiotherapy have been reported in other articles.[16]

Imaging techniques

Salivary gland scintigraphy was performed before initial treatment and then 3–5 months after completion of chemoradiotherapy. Salivary gland scintigraphy was performed with the gamma camera from a MillenniumVG system (GE Yokokawa Medical System, Milwaukee, WI). The only restriction before the examination was a dietary restriction. Dynamic imaging was obtained in a 64 × 64 pixel matrix at 15 s per frame for 45 min immediately after intravenous injection of 370 MBq of $^{99m}TcO_4^-$. Lemon juice (0.5 ml) was dripped into the oral cavity in 1800 s after intravenous injection as a taste stimulus. The energy window was ±10% around the 140 keV photopeak of ^{99m}Tc.

MRI was scheduled before initial treatment and then 3–5 months after completion of chemoradiotherapy. A 1.5-T system (Signa; GE Yokokawa Medical System) was used. Sequences comprised 3-dimensional spoiled gradient recalled acquisition in the steady state (3DSPGR) and saturation-transfer-prepared 3DSPGR (ST-3DSPGR). Single saturation transfer pulse (3.26 μT) frequency was employed at the frequency of 7 ppm downfield from the center frequency of water. Scans included the whole parotid gland. A neurovascular coil was used. Conditions were: repetition time, 40 ms; echo time, 6.9 ms; flip angle, 30°; bandwidth, 15.63 kHz; field of view, 24 cm; slice thickness, 5 mm; overlap locations, 0; locations per slab, 16; acquisition matrix, 512 × 126; and reconstructed matrix size, 512 × 512 (zerofill interoperation process). The stimulation of the parotid gland by for example lemon juice was not performed as in the scintigraphy protocol during MRI.

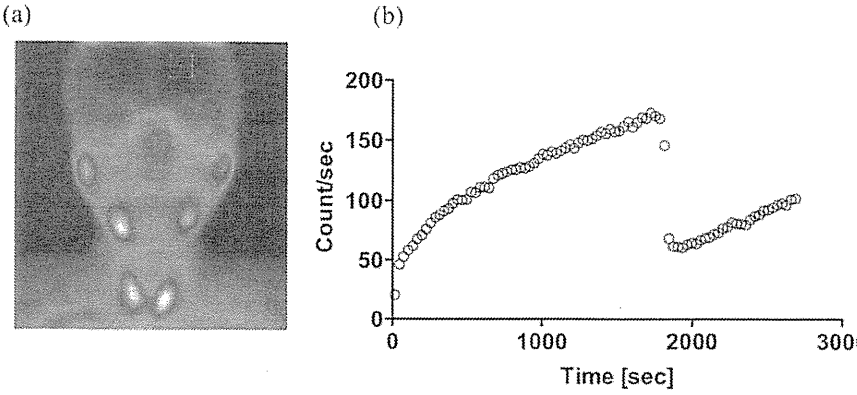

Fig. 1. (**a**) Planar image taken by salivary gland scintigraphy. ROIs were located for bilateral parotid glands and a frontal sinus. The count for the frontal sinus was used as the background level. (**b**) Representative time-activity curve (TAC) on a parotid gland. TAC on the parotid gland was created by subtracting background from the count for the gland.

Data analysis

Regions of interest (ROIs) were located for bilateral parotid glands and a frontal sinus on the planar image obtained by salivary gland scintigraphy (Fig. 1a), using the count for the frontal sinus as the background signal. A time-activity curve (TAC) for the parotid gland was created by subtracting the background from the count for the parotid gland (Fig. 1b). Maximum uptake rate (MUR) was calculated for bilateral parotid glands according to Equation 1.

$$MUR = (1 - C_{vpp} / C_{max}) \times 100\ [\%] \quad (1)$$

where C_{vpp} is the count on TAC at 60 s after administration of $^{99m}TcO_4^-$ (reflecting blood flow, capillary permeability and secretion rate in the parotid gland) and C_{max} is the maximum count on the TAC (reflecting capacities of blood vessel lumens and intercellular spaces in the parotid gland). MUR was used as the parameter indicating uptake function.

Washout rate (WOR) was calculated for bilateral parotid glands according to Equation 2.

$$WOR = (1 - C_{min} / C_{max}) \times 100\ [\%] \quad (2)$$

where C_{min} is the minimum counts after taste stimulation. WOR thus shows the secretion of $^{99m}TcO_4^-$ per capacities of blood vessel lumens and intercellular spaces in the parotid gland. WOR was used as the parameter indicating secretory function.

ECRI was obtained using Equation 3.

$$ECR = (M_0 / Ms - 1) \times 100\ [\%] \quad (3)$$

where Ms and M_0 represent signal intensities in 3DSPGR and ST-3DSPGR images, respectively. A ROI was located for the parotid gland on ECRI, and ECR at the parotid gland was measured.

We investigated correlations between ECR and both MUR and WOR at the parotid gland before and after chemoradiotherapy. Next, we investigated simple linear correlations between percentage changes in ECR, MUR and WOR at 3–5 months after chemoradiotherapy and median dose to the parotid gland.

Table 2. Changes in parameters

	Pre treatment series group (No. of parotid glands = 24)		Post treatment series group (No. of parotid glands = 24)
(a)			
MUR	74.7 ± 10.8	***	59.7 ± 8.1
WOR	61.0 ± 9.6	***	21.0 ± 16.5
(b)			
ECR values	30.0 ± 19.9	***	53.3 ± 22.5

Student's t test *** $p < 0.001$

Statistical analysis

R2.5.1 statistical software (www.r-project.org/) was used to perform all analyses. Student's t test was used to compare differences in patient groups. Pearson's correlation was used to evaluate correlations between ECR and MUR and between ECR and WOR at the parotid gland, and between percentage changes in ECR, MUR and WOR at 3–5 months after chemoradiotherapy and median dose to the parotid gland. The level of significance was set at 5%, and all p values were based on two-tailed tests.

RESULTS

Findings from salivary gland scintigraphy

Planar images taken by salivary gland scintigraphy were obtained in all cases without any acquisition failure. MUR and WOR could be obtained from all parotid glands on planar images. Table 2a shows changes in MUR and WOR

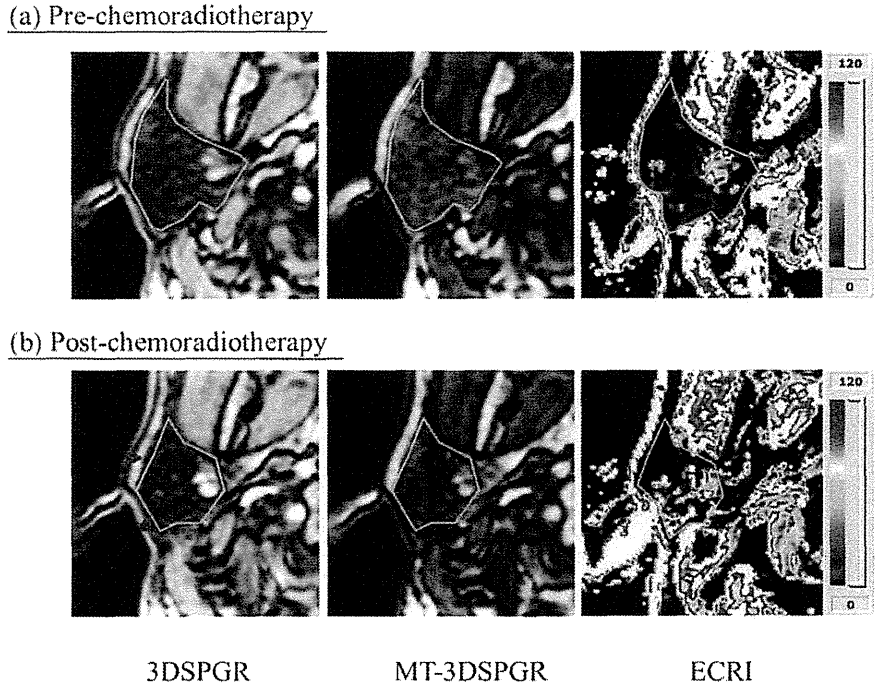

Fig. 2. Examples of 3DSPGR, MT-3DSPGR and ECR before (**a**) and after (**b**) chemoradiotherapy. Right parotid glands (areas surrounded by the yellow line) are shown in the axial plane. Volume reduction (indicated by arrowhead) was detected after chemoradiotherapy. ECRI was obtained using Equation 3.

between pre- and post-treatment groups. MUR was lower in the post-treatment group than in the pre-treatment group (Student's t test, $p < 0.001$). WOR was also lower in the post-treatment group than in the pre-treatment group (Student's t test, $p < 0.001$). Losses of uptake and secretory function in the parotid gland were thus confirmed by salivary gland scintigraphy.

Findings from ECRI

Both 3DSPGR and MT-3DSPGR images were obtained in all cases without any acquisition failure. ECR images were obtained using Equation 3. Figure 2 shows examples of 3DSPGR, MT-3DSPGR and ECR images before and after chemoradiotherapy. A clear reduction in parotid gland size after chemoradiotherapy was detected in this representative case (Fig. 2, arrowhead). ECR images were expressed in a graded color diagram of ECR values ranging from 0 to 120, with red indicating areas of high ECR, black showing areas of low ECR, and white representing areas with ECR > 120. Mean ECR values at parotid glands (± standard deviation) were 14.2 ± 0.72% and 34.3 ± 0.70% before and after chemoradiotherapy, respectively (Fig. 2). ECR values were higher in the post-treatment group than in the pre-treatment group (Table 2b; Student's t test, $p < 0.001$).

Correlations between ECR value and salivary gland scintigraphy parameters

To determine whether ECR values can be used to evaluate parotid gland function, we investigated correlations between ECR value and salivary gland scintigraphy parameters at the parotid gland. The correlation coefficient between ECR and MUR was –0.55 in the pre-treatment group (Pearson correlation, $p < 0.01$) and –0.50 in the post-treatment group (Pearson correlation, $p < 0.05$) (Fig. 3a). The correlation coefficients between ECR and WOR were –0.32 in the pre-treatment group (Pearson correlation, $p = 0.12$) and –0.06 in the post-treatment group (Pearson correlation, $p = 0.79$) (Fig. 3b).

Dose response

The 6 patients who underwent salivary gland scintigraphy and MRI both before and after chemoradiotherapy received a median dose of 19.8–26.5 Gy to the parotid glands (Table 3). The doses (several cGy per a MVCT acquisition) from the MVCT imaging were not contained in the median dose. Figure 4 shows the correlation between percentage change in parameters and median dose to the parotid gland. A significant correlation was identified between percentage change in ECR value at 3–5 months after chemoradiotherapy and median dose to the parotid gland (Pearson correlation, $r = -0.62$, $p < 0.05$). The correlation between percentage change

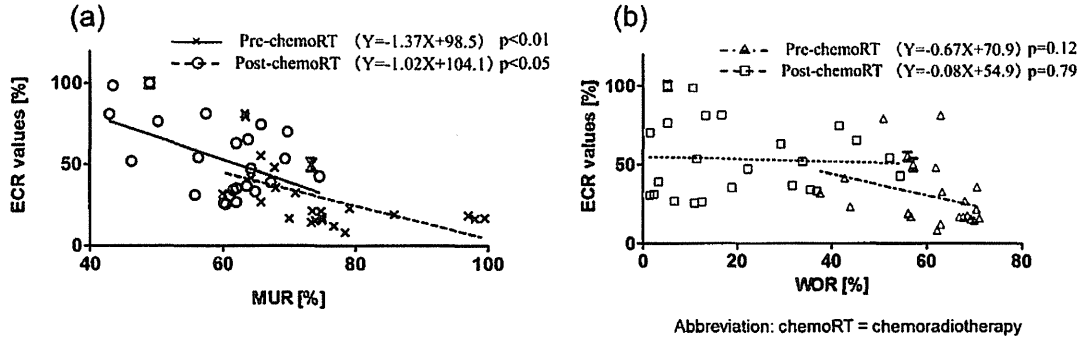

Fig. 3. Relationships between ECR value and salivary gland scintigraphy parameters. (a) MUR; (b) WOR.

Table 3. Median dose to parotid glands [Gy]

Patient No.	Right	Left
1	26.5	24.5
2	22.3	21.8
3	26.0	24.7
4	19.8	20.3
5	22.7	21.2
6	20.1	20.5

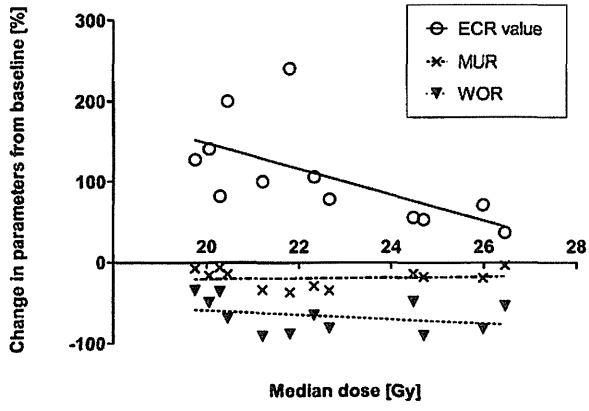

Fig. 4. Correlations between percentage change in parameters from baseline and median dose to parotid glands.

in MUR at 3–5 months after chemoradiotherapy and median dose to the parotid gland was not significant (Pearson correlation, r = 0.11, p = 0.74). The correlation between percentage change in WOR at 3–5 months after chemoradiotherapy and median dose to the parotid gland was also not significant (Pearson correlation, r = –0.31, p = 0.33).

DISCUSSION

Matsushima *et al.* previously reported ECRI as a potentially useful method for evaluating the efficacy of sentinel lymph node biopsy[9,10] and for cellular density imaging of axillary lymph nodes.[11] Yuen *et al.* reported ECRI as a feasible imaging technique for demonstrating breast cancer.[12] ECRI can thus detect minute changes in molecular and organizational structure.[8]

The present study represents the first trial of evaluating parotid gland function after chemoradiotherapy using ECRI. Parotid gland evaluation by MRI has been reported using ADC, which detects the motion of water molecules and microcirculatory blood flow.[5–7] Theony *et al.* reported that ADC value decreased immediately after taste stimulation, then increased until static state.[5] Dirix *et al.* reported that ADC value decreased significantly after irradiation.[6] Likewise, Lin *et al.* reported that ADC value decreased significantly after irradiation, and correlated with parameters obtained by salivary scintigraphy (uptake rate; $r = 0.36$, $p < 0.01$, MUR; $r = 0.33$, $p < 0.01$).[7] In our results, correlation coefficients between ECR and MUR were –0.55 ($p < 0.01$) in the pre-treatment group and –0.50 ($p < 0.05$) in the post-treatment group. The correlation coefficient between ECR and MUR was higher than that between ADC and MUR in past studies.[7] The reason why ECR correlated with MUR before chemoradiotherapy is as follows. When capacities of blood vessel lumens and intercellular spaces are large, C_{vpp} / C_{max} is low, and MUR (defined as $1 - C_{vpp} / C_{max}$) is high. Conversely, cell densities are relatively decreased, and the ECR (expressing cell density) is thus low. ECR thus showed a negative correlation with MUR. Moreover, ECR showed a correlation with MUR in the post-treatment group for the following reasons. Animal experiments have identified shrinkage of irradiated parotid glands.[17] Likewise, the parotid gland after chemoradiotherapy shrank in the present study (Fig. 2). ECR shows a high value due to the rise in cell density, while MUR was low due to decreased free water and the narrowness of the free water division, with shrinkage of gland tissues. ECR therefore shows a negative correlation with MUR in the post-treatment group. This relationship suggests that ECR value can be used to evaluate uptake function of the parotid gland after chemoradiotherapy without exposure to radiation. In addition, as ECRI can provide

a 2-dimensional color map (Fig. 2), areas of weak uptake function in the parotid gland can be identified visually. The details of mechanism for the uptake of saliva are unknown. Therefore, the visualization of uptake function may contribute for the clarification of the loss part of uptake function of saliva. The correlation coefficients between ECR and WOR were –0.32 in the pre-treatment group (Pearson correlation, $p = 0.12$) and –0.06 in the post-treatment group (Pearson correlation, $p = 0.79$) (Fig. 3b). However, as the stimulation of the parotid gland by for example lemon juice was not performed as in the scintigraphy protocol during MRI, both exams could not be compared.

On salivary scintigraphy, dose-response with parotid gland function has been studied by other investigators,[1–3,18–20] Roesink *et al.* found a significant correlation between salivary excretion factor (defined as the percentage of activity in the parotid gland that disappeared within 15 min following administration of carbachol) and mean radiation dose to the parotid glands.[3] However, in our research, WOR did not show a linear correlation with radiation dose to the parotid glands (Fig. 4). This lack of correlation may be due to low number of patients and differences in dose ranges applied in this study. Moreover, the difference between median and mean doses might be involved. On the other hand, calculations of secretory functions (such as salivary excretion factor and WOR) and uptake functions (such as MUR) have been widely recognized for salivary scintigraphy. However, dose-response for uptake function has not been reported. In our research, the percentage change in MUR at 3–5 months after chemoradiotherapy did not show a linear correlation with median radiation dose to the parotid gland (Pearson correlation, $r = 0.11$, $p = 0.74$). Conversely, the percentage change in ECR values at 3–5 months after chemoradiotherapy showed a linear correlation with median radiation dose to the parotid gland (Pearson correlation, $r = -0.62$, $p < 0.05$). ECR thus showed a linear correlation with median radiation dose to parotid glands in the range of 19.8–26.5 Gy. The reason why ECR correlates with median radiation dose to the parotid gland can be described as follows from the perspective of cell density. In this research, cell-density-weighted images were obtained by irradiating the saturation pulse at a frequency 7 ppm downfield from the center frequency of water. Matsushima *et al.* reported that ECR correlated with cell density in clinical situations.[11] In addition, the number of acinar cells is known to be decreased in irradiated salivary gland.[21–27] Li *et al.* reported that the number of acinar cells in irradiated parotid glands was decreased at 16 weeks after radiotherapy.[27] This duration after radiotherapy is similar to that used in our research. Loss of acinar cells is markedly increased with increasing dose to the parotid gland.[26,27] The percentage change in ECR values at 3–5 months after chemoradiotherapy thus shows a clear inverse correlation with median radiation dose to the parotid gland. This suggests that ECR value can be used to predict uptake function of the parotid gland after chemoradiotherapy.

In conclusion, we verified that ECRI is useful for evaluating parotid gland function after chemoradiotherapy. ECRI allowed visual evaluation of uptake function in the parotid gland without exposure to radiation.

ACKNOWLEDGEMENTS

We are indebted to Masataka Murakami at National Institute for Physiological Sciences and Seiichi Era at Gifu University Graduate School of Medicine for many helpful discussions in the course of this investigation.

REFERENCES

1. Munter MW, *et al* (2007) Changes in salivary gland function after radiotherapy of head and neck tumors measured by quantitative pertechnetate scintigraphy: comparison of intensity-modulated radiotherapy and conventional radiation therapy with and without Amifostine. Int J Radiat Oncol Biol Phys **67**(3): 651–659.
2. Bussels B, *et al* (2004) Dose-response relationships within the parotid gland after radiotherapy for head and neck cancer. Radiother Oncol **73**(3): 297–306.
3. Roesink JM, *et al* (2004) Scintigraphic assessment of early and late parotid gland function after radiotherapy for head-and-neck cancer: a prospective study of dose-volume response relationships. Int J Radiat Oncol Biol Phys **58**(5): 1451–1460.
4. ICRP Publication 53 (1987) Radiation dose to patients from radiopharmaceuticals.
5. Thoeny HC, *et al* (2005) Gustatory stimulation changes the apparent diffusion coefficient of salivary glands: initial experience. Radiology **235**(2): 629–634.
6. Dirix P, *et al* (2008) Diffusion-weighted magnetic resonance imaging to evaluate major salivary gland function before and after radiotherapy. Int J Radiat Oncol Biol Phys **71**(5): 1365–1371.
7. Zhang L, *et al* (2001) Yoshimura R, Shibuya H. Functional evaluation with intravoxel incoherent motion echo-planar MRI in irradiated salivary glands: a correlative study with salivary gland scintigraphy. J Magn Reson Imaging **14**(3): 223–229.
8. Sogami M, *et al* (2001) Basic studies on the equivalent cross-relaxation rate imaging (equivalent CRI)--phantom studies. NMR Biomed **14**(6): 367–375.
9. Matsushima S, *et al* (2005) Equivalent cross-relaxation rate imaging for sentinel lymph node biopsy in breast carcinoma. Magn Reson Med **54**(5): 1300–1304.
10. Matsushima S, *et al* (2003) Equivalent cross relaxation rate image for decreasing a false negative case of sentinel lymph node biopsy. Magn Reson Imaging **21**(9): 1045–1047.
11. Mastsushima S, *et al* (2008) Equivalent cross-relaxation rate imaging of axillary lymph nodes in breast cancer. J Magn Reson Imaging **27**(6): 1278–1283.
12. Yuen S, *et al* (2004) Equivalent cross-relaxation rate imaging of breast cancer. J Magn Reson Imaging **20**(1): 56–65.
13. Fleming ID, Cooper JS and Henson DE (1997) AJCC cancer staging manual. 5th ed. Philadelphia: J. B. Lippincott.

14. Forrest LJ, *et al* (2004) The utility of megavoltage computed tomography images from a helical tomotherapy system for setup verification purposes. Int J Radiat Oncol Biol Phys **60**(5): 1639–1644.
15. Langen KM, *et al* (2005). Initial experience with megavoltage (MV) CT guidance for daily prostate alignments. Int J Radiat Oncol Biol Phys **62**(5): 1517–1524.
16. Fuwa N, *et al* (2002) Phase I study of combination chemotherapy with 5-fluorouracil (5-FU) and nedaplatin (NDP): adverse effects and eecommended dose of NDP administered after 5-FU. Am J Clin Oncol **25**(6): 565–569.
17. Vasquez Osorio EM, *et al* (2008) Local anatomic changes in parotid and submandibular glands during radiotherapy for oropharynx cancer and correlation with dose, studied in detail with nonrigid registration. Int J Radiat Oncol Biol Phys **70**(3): 875–882.
18. van Acker F, *et al* (2001) The utility of SPECT in determining the relationship between radiation dose and salivary gland dysfunction after radiotherapy. Nucl Med Commun **22**(2): 225–231.
19. Tenhunen M, *et al* (2008) Scintigraphy in prediction of the salivary gland function after gland-sparing intensity modulated radiation therapy for head and neck cancer. Radiother Oncol **87**(2): 260–267.
20. Maes A, *et al* (2002) Preservation of parotid function with uncomplicated conformal radiotherapy. Radiother Oncol **63**(2): 203–211.
21. Price RE, *et al* (1995) Effects of continuous hyperfractionated accelerated and conventionally fractionated radiotherapy on the parotid and submandibular salivary glands of rhesus monkeys. Radiother Oncol **34**(1): 39–46.
22. Coppes RP, Vissink A and Konings AW (2002) Comparison of radiosensitivity of rat parotid and submandibular glands after different radiation schedules. Radiother Oncol **63**(3): 321–328.
23. Urek MM, *et al* (2005) Early and late effects of X-irradiation on submandibular gland: a morphological study in mice. Arch Med Res **36**(4): 339–343.
24. Cooper JS, *et al* (1995) Late effects of radiation therapy in the head and neck region. Int J Radiat Oncol Biol Phys **31**(5): 1141–1164.
25. Konings AW, Coppes RP and Vissink A (2005) On the mechanism of salivary gland radiosensitivity. Int J Radiat Oncol Biol Phys **62**(4): 1187–1194.
26. Muhvic-Urek M, *et al* (2006) Imbalance between apoptosis and proliferation causes late radiation damage of salivary gland in mouse. Physiol Res **55**(1): 89–95.
27. Li J, *et al* (2005) Structural and functional characteristics of irradiation damage to parotid glands in the miniature pig. Int J Radiat Oncol Biol Phys **62**(5): 1510–1516.

Received on April 11, 2011
Revision received on October 4, 2011
Accepted on October 5, 2011

J Cancer Res Clin Oncol (2012) 138:1931–1936
DOI 10.1007/s00432-012-1277-0

ORIGINAL PAPER

Preliminary results of intensity-modulated radiation therapy with helical tomotherapy for prostate cancer

Natsuo Tomita · Norihito Soga · Yuji Ogura · Norio Hayashi · Hidetoshi Shimizu · Takashi Kubota · Junji Ito · Kimiko Hirata · Yukihiko Ohshima · Hiroyuki Tachibana · Takeshi Kodaira

Received: 5 May 2012 / Accepted: 21 June 2012 / Published online: 1 July 2012

Abstract
Purpose We present the preliminary results of intensity-modulated radiation therapy with helical tomotherapy (HT) for clinically localized prostate cancer.
Methods Regularly followed 241 consecutive patients, who were treated with HT between June 2006 and December 2010, were included in this retrospective study. Most patients received both relatively long-term neoadjuvant and adjuvant androgen deprivation therapy (ADT). Patients received 78 Gy in the intermediate high-risk group and 74 Gy in the low-risk group. Biochemical disease-free survival (bDFS) followed the Phoenix definition. Toxicity was scored according to the Radiation Therapy Oncology Group morbidity grading scale.
Results The median follow-up time from the start date of HT was 35 months. The rates of acute Grade 2 gastrointestinal (GI) and genitor-urinary (GU) toxicities were 11.2 and 24.5 %. No patients experienced acute Grade 3 or higher symptoms. The rates of late Grade 2 and 3 GI toxicities were 6.6 and 0.8 %, and those of late Grade 2 and 3 GU toxicities were 8.3 % and 1.2 %. No patients experienced late Grade 4 toxicity. The 3-year bDFS rates for low, intermediate, and high-risk group patients were 100, 100, and 95.8 %, respectively. We observed clinical relapse in two high-risk patients, resulting in a 3-year clinical DFS of 99.4 %.
Conclusions This preliminary report confirms the feasibility of HT in a large number of patients. We observed that HT is associated with low rates of acute and late toxicities, and HT in combination with relatively long-term ADT results in excellent short-term bDFS.

Keywords Prostate cancer · Intensity-modulated radiation therapy · Image-guided radiation therapy · Helical tomotherapy

N. Tomita (✉) · H. Shimizu · T. Kubota · J. Ito · K. Hirata · Y. Ohshima · H. Tachibana · T. Kodaira
Department of Radiation Oncology, Aichi Cancer Center Hospital, 1-1 Kanokoden, Chikusaku, Nagoya 464-8681, Japan
e-mail: ntomita@aichi-cc.jp

N. Soga · Y. Ogura · N. Hayashi
Department of Urology, Aichi Cancer Center Hospital, Nagoya, Japan

Introduction

High-dose external beam radiation therapy (EBRT) with intensity-modulated radiation therapy (IMRT) has been shown to improve disease-free survival in patients with localized prostate cancer over the past decade (Zelefsky et al. 2002; Alicikus et al. 2011). Helical tomotherapy (HT) is a novel IMRT treatment modality. HT is a form of 3D conformal radiation therapy in which treatment beams are spatially and temporally modulated to maximize the dose delivered to tumors while minimizing the dose delivered to normal structures (Kapatoes et al. 2001). In addition, detectors within the tomotherapy system provide megavoltage computed tomographic (MVCT) images of the patient, which can be obtained immediately before treatment for setup, registration, and repositioning [i.e., image-guided radiation therapy (IGRT)]. Thus, we believe that HT provides excellent target coverage with dose uniformity while sparing the organs at risk (OAR) and would avoid severe toxicity in patients with prostate cancer. On the other hand, IMRT has been used in Japan recently, especially for prostate cancer. However, to our knowledge, Japanese data of prostate cancer treated with IMRT have not been reported. In this report, we present the preliminary

results of IMRT with HT for clinically localized prostate cancer in Japan.

Materials and methods

Patients

Between June 2006 and December 2010, 251 patients with clinically localized prostate cancer were treated with HT at our institution. Of these, 10 patients were followed at their local hospital. Another 241 consecutive patients, who were followed regularly at our institution, were included in this retrospective study. Pretreatment diagnostic evaluations were performed by serum prostate-specific antigen (PSA), digital rectal examination, magnetic resonance imaging of the pelvis, computed tomography (CT) of the chest to the pelvis, and bone scintigraphy. All patients had histological diagnosis of prostatic adenocarcinoma, classified according to the Gleason grading system. The American Joint Committee on Cancer 2002 clinical staging was used, and patients were classified into three prognostic risk groups defined by the National Comprehensive Cancer Network criteria (http://www.nccn.org/) as follows: low, pretreatment PSA < 10 ng/ml, T1–T2a, and Gleason score ≤ 6; intermediate, T2b–T2c or Gleason score 7 or PSA 10–20 ng/ml; high, T3a or Gleason score 8–10 or PSA > 20 ng/ml. We classified patients with T3b–T4 clinical stage as a high-risk group in this study. Table 1 describes patient characteristics.

Table 1 Patient characteristics

Characteristic	$n = 241$
Age (years)	69 (49–81)
PSA level (ng/ml)	
<10	79 (32.8 %)
10–20	65 (27.0 %)
>20	97 (40.2 %)
Median	15.17
Range	1.40–502.00
Gleason score	
2–6	47 (19.5 %)
7	97 (40.2 %)
8–10	97 (40.2 %)
Tumor stage	
T1–T2a	73 (30.3 %)
T2b–T2c	36 (14.9 %)
T3a	97 (40.2 %)
T3b–T4	35 (14.6 %)
Risk group	
Low	17 (7.0 %)
Intermediate	53 (22.0 %)
High	171 (71.0 %)

Age data are presented as median values

Hormonal therapy

All patients were given neoadjuvant androgen deprivation therapy (N-ADT). A combination of a luteinizing hormone releasing hormone (LHRH) analogue and anti-androgen treatment (i.e., maximum androgen blockade) was performed as N-ADT. N-ADT time depended on the IMRT reservation in principle, and the median time of N-ADT was 9 months (range 2–68 months). Adjuvant ADT (A-ADT) consisted of only the LHRH analogue. Patients were given A-ADT for 1–2 years at the discretion of the urologists. Eight patients (3.3 %) did not receive A-ADT because they experienced adverse effects associated with N-ADT such as liver dysfunction, and 29 patients (12.0 %) continue to receive A-ADT at the time of this analysis. The median time of A-ADT in another patient was 20 months (range 1–37 months).

IMRT treatment

All patients were immobilized in a supine position with the Esform vacuum type immobilization system (Engineering System, Matsumoto, Japan) and simulated by pelvic computed tomography (CT) with a 2.5-mm slice thickness. On the day of CT simulation and during IMRT, all patients defecated where possible every morning and discharged urine about one hour before CT simulation and IMRT to minimize daily variations in the shape and anatomical location of the prostate. Outlines of the target were delineated on a 3-dimensional radiation treatment planning system (Pinnacle3 workstation, Hitachi Medical Corporation, Tokyo, Japan) using the abdominal CT window setting. Clinical target volume (CTV) was defined as the entire prostate and proximal seminal vesicle. In the case of seminal vesicle invasion, CTV included the entire seminal vesicle. Planning target volume 1 (PTV1) included CTV with a 6–8 mm margin except at the prostatorectal interface, where a 4–6 mm margin was used. PTV2 was defined as the seminal vesicle with a similar margin as PTV1 outside of PTV1. Normal structures including the rectum, bladder, femoral head, penile bulb, pubic bone, bowel, and sigmoid colon adjacent to PTV were considered to be OAR. The rectum was delineated only around PTV1 with 10 mm on the cranio-caudal direction. CT images and structure sets were transferred to the Tomotherapy Hi-Art System workstation (TomoTherapy Inc., Madison, WI, USA). Normal structures were constrained on an individual basis using maximum and dose–volume histogram (DVH) dose constraints without compromising PTV1 coverage.

The dose constraints required to achieve an acceptable HT plan in our institution were as follows: (1) PTV1 D95 (i.e., dose delivered to 95 % of PTV1): 74 Gy in the low-risk group, 78 Gy in intermediate and high-risk groups, maximum dose < 107 % of the prescribed dose, minimum dose > 90 % of the prescribed dose; (2) PTV2 D95: 64 Gy, minimum dose > 90 % of the prescribed dose; (3) rectum: the percentage of the entire rectum covered by at least 70 Gy (V70) < 15 %, V60 < 25 %, and V40 < 45 %; (4) bladder: the percentage of the entire bladder covered by at least 60 Gy (V60) < 25 % and V40 < 50 %; (5) femoral head: maximum dose < 40 Gy; (6) bowel, sigmoid colon: the volume covered by 55 Gy < 0.5 cc; (7) penile bulb: mean dose < 52.5 Gy; and (8) pubic bone: V70 < 20 %.

In tomotherapy treatment conditions, a 2.5-cm field width was used in all patients. Other common parameters were a pitch of 0.430 and a normal modulation factor of 2.0. The inverse planning system performed a variable number of iterations, which ranged from 100 to 300, during the optimization process for each plan. All patients began treatment with daily MVCT acquisitions for setup, registration, and repositioning on the basis of the location of the prostate. Patients inserted a tube or were encouraged to defecate when their rectums were dilated on MVCT and were checked on MVCT again.

Follow-up

Follow-up evaluations after treatment were performed at intervals of 3 months. Serum PSA was measured at each follow-up. The length of follow-up was calculated from the start date of IMRT. Biochemical disease-free survival (bDFS) followed the Phoenix definition (i.e., a post-treatment nadir plus 2.0 ng/ml Roach et al. 2006). A clinical relapse comprised local disease, and lymph node, bone, or parenchymal metastases detected by CT scan and/or bone scintigraphy. Patients began ADT again after documentation of biochemical relapse. Distributions of bDFS, disease-free survival (DFS), and overall survival were calculated according to the Kaplan–Meier method. The Student's t test was used in the analysis of prognostic factors for biochemical control. A p value of <0.05 was considered significant. Toxicity was scored according to the Radiation Therapy Oncology Group morbidity grading scale (Cox et al. 1995). In brief, Grade 1 toxicity represents minimal side effects not requiring medication for symptom control, Grade 2 toxicity indicates symptoms requiring medication, Grade 3 indicates complications requiring minor surgical intervention (i.e., transurethral resection, laser coagulation, or blood transfusion), and Grade 4 requires hospitalization and major intervention. The time to develop late toxicity was the interval from the start date of IMRT.

Results

The prescribed dose was slightly reduced to 74 or 70 Gy in 16 patients (6.6 %) because of their antithrombogenic medications (6 patients), failure in OAR dose constraints (4 patients, especially in those whose bowel or sigmoid colon invaginated into the surrounding area of PTV1), patients' request or physicians' suggestion for their acute rectal symptoms (3 patients), financial reasons (one patient), and unspecified in 2 patients. The median IMRT period was 57 days (range 51–95 days). The median follow-up time from the start date of IMRT was 35 months (range 13–66 months).

Acute toxicity

Table 2 shows the incidence of acute gastro-intestinal (GI) and genitor-urinary (GU) toxicities treated with IMRT with HT. Of 27 patients (11.2 %) who developed acute Grade 2 rectal toxicity requiring medication such as suppositories, the main symptoms were pain on defecation in 17 patients (7.1 %) and rectal bleeding with bowel movements in 10 patients (4.1 %), respectively. Of 59 patients (24.5 %) who developed acute Grade 2 urinary toxicity, most symptoms (55, 22.7 %) were dysuria such as urinary frequency, and other symptoms were gross hematuria in 3 patients (1.2 %) and pain with urination in 2 patients (0.8 %). No patients experienced acute Grade 3 or higher acute symptoms.

Late toxicity

The incidence of late GI and GU toxicities is also shown in Table 2. Of 16 patients (6.6 %) who developed late Grade 2 rectal toxicity, 13 patients (5.4 %) developed Grade 2 rectal bleeding at a median of 18 months (range 10–39 months) after the start date of IMRT. Other symptoms were pain on defecation in 2 patients (0.8 %) after 9 and 11 months and subtle fecal incontinence in one patient (0.4 %) after 9 months. Two patients (0.8 %) developed Grade 3 rectal bleeding requiring laser coagulation at 11

Table 2 Incidence of acute and late Grade 2 or higher gastro-intestinal (GI) and genitor-urinary (GU) toxicity among patients treated with intensity-modulated radiation therapy (IMRT) with helical tomotherapy ($n = 241$)

	Acute toxicity		Late toxicity	
	GI	GU	GI	GU
Grade 2	27 (11.2 %)	59 (24.5 %)	16 (6.6 %)	20 (8.3 %)
Grade 3	0 (0 %)	0 (0 %)	2 (0.8 %)	3 (1.2 %)
Grade 4	0 (0 %)	0 (0 %)	0 (0 %)	0 (0 %)
Total	27 (11.2 %)	59 (24.5 %)	18 (7.4 %)	23 (9.5 %)

Table 3 Patient characteristics with or without biochemical relapse after intensity-modulated radiation therapy (IMRT) with helical tomotherapy

Characteristic	Biochemical relapse group ($n = 6$)	Biochemical control group ($n = 169$)	p value
Age (years)	65 (51–77)	69 (49–81)	0.041
PSA level (ng/ml)	38.26 (24.88–153.00)	15.17 (1.40–502.00)	0.057
Gleason score	9 (8–10)	7 (5–10)	0.0030
Tumor stage			0.00022
T1–T2c	0 (0 %)	82 (50.3 %)	
T3a	2 (33.3 %)	63 (38.7 %)	
T3b–T4	4 (66.7 %)	18 (11.0 %)	
Risk group			0.13
Low	0 (0 %)	14 (8.2 %)	
Intermediate	0 (0 %)	39 (23.0 %)	
High	6 (100 %)	113 (68.8 %)	

and 12 months after the start date of IMRT. No Grade 4 late rectal complications have been observed. Of 20 patients (8.3 %) who developed late Grade 2 urinary toxicity, 16 patients (6.6 %) experienced dysuria requiring medication at a median of 19 months (range 7–47 months) after the start date of IMRT. Other symptoms were gross hematuria in 2 patients (0.8 %) and cystitis in 2 patients (0.8 %). Two patients (0.8 %) experienced Grade 3 urinary retention requiring self-catheterization or dilation at 14 and 17 months after the start date of IMRT. One patient developed a bladder ulcer (Grade 3) requiring laser coagulation after 14 months. No patients experienced late Grade 4 urinary symptoms.

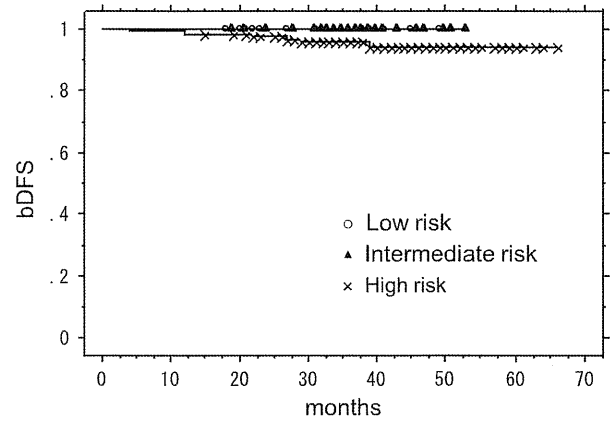

Fig. 1 The 3-year biochemical disease-free survival (bDFS) for low, intermediate, and high-risk group patients

Biochemical control, clinical relapse, and overall survival

Biochemical control was estimated in only 175 patients followed for at least 6 months after the completion of A-ADT. Six patients in the high-risk group developed biochemical relapse at a median of 25 months (range 4–39) after the start date of IMRT. No patients in low and intermediate risk groups experienced biochemical relapse. Table 3 shows each patient's characteristics with or without biochemical relapse. Age, Gleason score, and T-stage were significant factors of biochemical relapse in patient characteristics ($p = 0.041$, 0.0030, and 0.00022, respectively). PSA in the biochemical relapse group seemed to be higher than those in the biochemical control group, but PSA and the risk group had no significant impact on the biochemical control.

The 3-year bDFS rate was 96.9 % (95 % confidence interval (CI): 94.2–99.6 %) in all groups. The 3-year bDFS rates for low, intermediate, and high-risk group patients were 100, 100, and 95.8 % (CI: 92.1–99.5 %), respectively. The bDFS for each risk group are shown in Fig. 1. We observed clinical relapse in two patients in the high-risk group, resulting in a 3-year clinical DFS of 99.4 % (CI: 98.2–100 %). One patient developed bone metastasis of the humerus after 4 months, and the other patient developed pelvic node metastases after 39 months. Each patient received ADT after clinical relapse. No patient died at the time of analysis, resulting in a 3-year OS of 100 %.

Discussion

We could not find a published report for Japanese outcomes of prostate cancer treated with IMRT in a PubMed search, although there were many reports of permanent brachytherapy. Therefore, to our knowledge, this data may be the first report to compile IMRT-treated patients in Japan and demonstrate the feasibility of high-dose radiotherapy with HT for patients with localized prostate cancer. Localized prostate cancer patients, especially those in the low-risk group, usually have some radical treatment choices such as radical prostatectomy, IMRT, brachytherapy, particle therapy, and recently implemented robotic surgery. This report provided outcomes and toxicities for localized

prostate cancer after IMRT with IGRT (i.e., HT) combined with ADT in one of the Japanese cancer centers, and this could be the basis of comparison with other treatments and will be of assistance for patients and physicians associated with prostate cancer at the time for treatment choice.

Most patients could receive the prescribed total doses, but they were slightly reduced in 16 patients (6.6 %). To our knowledge, the impact of antithrombogenic medication on GI toxicity is still uncertain. The total doses of some patients who took this medication were reduced based on each physician's clinical decision. We will estimate the impact of the antithrombogenic medication on toxicity circumstantially in the near future. Some patients received a reduced total dose because of their acute rectal symptoms. Zelefsky et al. (2008) recently reported that the presence of acute GI and GU symptoms during treatment conferred a fivefold and threefold increased risk of late GI and GU toxicities, respectively, in 1,571 patients with prostate cancer who had a long follow-up after receiving 3-dimensional conformal radiotherapy (3DCRT) or IMRT. Therefore, we think that these patients would have developed severe late GI toxicity if they had received the prescribed total dose. We will also estimate the relationship between acute and late toxicity for patients treated with HT. We reduced the total dose for some patients due to failure in OAR dose constraints, especially in patients whose bowel or sigmoid colon invaginated into the surrounding area of PTV1. We think that these patients should choose other treatments such as surgery if possible.

We observed a satisfactory low rate in acute GI and GU toxicity, and the Grade 2 rates of acute GI and GU toxicity were 11.2 and 24.5 %, respectively. Among patients who developed acute Grade 2 rectal toxicity, the main symptoms were pain on defecation. We think from our clinical experience that these symptoms were not so much due to the doses exposed to the rectum, but rather too much effort from each patient's to empty their bowels because they had inserted a tube or were encouraged to defecate when their rectums were dilated on MVCT. On the other hand, we observed a satisfactory low rate in late GI and GU toxicity, and the rates of late Grade 2 or higher GI and GU toxicity were only 7.4 and 9.5 %, respectively. Data indicate that late rectal toxicity profiles are excellent compared to the incidence of late Grade 2 or higher GU and GI toxicity that reportedly ranged from 24 to 35 % and from 15 to 29 %, respectively, in recent studies with the use of IMRT (Vora et al. 2007; Wong et al. 2009; Sharma et al. 2011). We think that our favorable toxicity rates came partly as a result of IGRT with HT. The significance of IGRT is established in EBRT for localized prostate cancer (http://www.nccn.org/). However, IGRT was conducted at only approximately 60 % of facilities in a recent Japanese national survey on the current status of EBRT for prostate cancer (Nakamura et al. 2012). Another may be the relatively tight margin used between CTV and PTV. Enmark et al. (2006) demonstrated that a margin of 4 mm in all directions was adequate to account for uncertainties including inter- and intra-fraction motions. In a recent report (Crehange et al. 2012), 165 men were treated with daily IMRT with IGRT using a 3D ultrasound-based system and stratified regarding CTV to PTV margin: group A, 5 mm or group B, 10 mm. Their data indicated that the margin had no impact on short-term bDFS in control of IGRT. We also confirmed favorable short-term bDFS in the current report. However, long-term follow-up is required to evaluate the clinical significance of the tight margin with IGRT.

Our preliminary results suggest excellent short-term biochemical out-comes for all risk group patients when treated with HT combined with relatively long-term ADT. Of course, longer follow-up will be necessary to determine whether HT results in an incremental favorable outcome in tumor control. Actually, in our clinical experience of 3DCRT (Tomita et al. 2009), patients develop biochemical relapse 4–5 years after the start date of RT when combined with long-term (>2 years) ADT. All patients who developed biochemical relapse were in the high-risk group in this cohort, and age, Gleason score, and T-stage were significant factors of biochemical relapse in patient characteristics. Ogawa et al. (2011) surveyed the pattern of care study (PCS) for radical EBRT for clinically localized prostate cancer in Japan. They reported that the number of patients in the high-risk group consisted of more than 60 % of the 2003–2005 survey, although the number of patients in the high-risk group decreased gradually. The current study cohort was similar to that of PCS. There is room for consideration of the treatment strategy for high-risk prostate cancer patients in Japan.

In conclusion, this preliminary report confirms the feasibility of HT in a large number of localized prostate cancer patients. We observed that HT is associated with low rates of acute and late toxicities, and HT in combination with relatively long-term ADT results in excellent short-term bDFS. Superior dose distributions and IGRT with HT are better options not only for high-dose EBRT, but also for all treatment choices of localized prostate cancer.

Conflict of interest We declare that we have no conflict of interest.

References

Alicikus ZA, Yamada Y, Zhang Z, Pei X, Hunt M, Kollmeier M, Cox B, Zelefsky MJ (2011) Ten-year outcomes of high-dose, intensity-modulated radiotherapy for localized prostate cancer. Cancer 117(7):1429–1437

Cox JD, Stetz J, Pajak TF (1995) Toxicity criteria of the Radiation Therapy Oncology Group (RTOG) and the European Organization for Research and Treatment of Cancer (EORTC). Int J Radiat Oncol Biol Phys 31(5):1341–1346

Crehange G, Mirjolet C, Gauthier M, Martin E, Truc G, Peignaux-Casasnovas K, Azelie C, Bonnetain F, Naudy S, Maingon P (2012) Clinical impact of margin reduction on late toxicity and short-term biochemical control for patients treated with daily online image guided IMRT for prostate cancer. Radiother Oncol 103(2):244–246

Enmark M, Korreman S, Nystrom H (2006) IGRT of prostate cancer; is the margin reduction gained from daily IG time-dependent? Acta Oncol 45(7):907–914

Kapatoes JM, Olivera GH, Ruchala KJ, Smilowitz JB, Reckwerdt PJ, Mackie TR (2001) A feasible method for clinical delivery verification and dose reconstruction in tomotherapy. Med Phys 28(4):528–542

Nakamura K, Akimoto T, Mizowaki T, Hatano K, Kodaira T, Nakamura N, Kozuka T, Shikama N, Kagami Y (2012) Patterns of practice in intensity-modulated radiation therapy and image-guided radiation therapy for prostate cancer in Japan. Jpn J Clin Oncol 42(1):53–57

National Comprehensive Cancer Network. NCCN clinical practice guidelines in oncology: prostate cancer V1 2011. http://www.nccn.org/. Accessed 10 April 2012

Ogawa K, Nakamura K, Sasaki T, Onishi H, Koizumi M, Araya M, Mukumoto N, Teshima T, Mitsumori M (2011) Radical external beam radiotherapy for clinically localized prostate cancer in Japan: changing trends in the patterns of care process survey. Int J Radiat Oncol Biol Phys 81(5):1310–1318

Roach M 3rd, Hanks G, Thames H Jr, Schellhammer P, Shipley WU, Sokol GH, Sandler H (2006) Defining biochemical failure following radiotherapy with or without hormonal therapy in men with clinically localized prostate cancer: recommendations of the RTOG–ASTRO phoenix consensus conference. Int J Radiat Oncol Biol Phys 65(4):965–974

Sharma NK, Li T, Chen DY, Pollack A, Horwitz EM, Buyyounouski MK (2011) Intensity-modulated radiotherapy reduces gastrointestinal toxicity in patients treated with androgen deprivation therapy for prostate cancer. Int J Radiat Oncol Biol Phys 80(2):437–444

Tomita N, Kodaira T, Tachibana H, Nakamura T, Tomoda T, Nakahara R, Inokuchi H, Hayashi N, Fuwa N (2009) Dynamic conformal arc radiotherapy with rectum hollow-out technique for localized prostate cancer. Radiother Oncol 90(3):346–352

Vora SA, Wong WW, Schild SE, Ezzell GA, Halyard MY (2007) Analysis of biochemical control and prognostic factors in patients treated with either low-dose three-dimensional conformal radiation therapy or high-dose intensity-modulated radiotherapy for localized prostate cancer. Int J Radiat Oncol Biol Phys 68(4):1053–1058

Wong WW, Vora SA, Schild SE, Ezzell GA, Andrews PE, Ferrigni RG, Swanson SK (2009) Radiation dose escalation for localized prostate cancer: intensity-modulated radiotherapy versus permanent transperineal brachytherapy. Cancer 115(23):5596–5606

Zelefsky MJ, Fuks Z, Hunt M, Yamada Y, Marion C, Ling CC, Amols H, Venkatraman ES, Leibel SA (2002) High-dose intensity modulated radiation therapy for prostate cancer: early toxicity and biochemical outcome in 772 patients. Int J Radiat Oncol Biol Phys 53(5):1111–1116

Zelefsky MJ, Levin EJ, Hunt M, Yamada Y, Shippy AM, Jackson A, Amols HI (2008) Incidence of late rectal and urinary toxicities after three-dimensional conformal radiotherapy and intensity-modulated radiotherapy for localized prostate cancer. Int J Radiat Oncol Biol Phys 70(4):1124–1129

Journal of Radiation Research, 2012, 53, 906–915
doi: 10.1093/jrr/rrs052 Advance Access Publication 22 July 2012

Treatment outcomes of definitive chemoradiotherapy for patients with hypopharyngeal cancer

Rie NAKAHARA[1,2,*], Takeshi KODAIRA[1], Kazuhisa FURUTANI[1], Hiroyuki TACHIBANA[1], Natsuo TOMITA[1], Haruo INOKUCHI[1], Nobutaka MIZOGUCHI[1], Yoko GOTO[1], Yoshiyuki ITO[2] and Shinji NAGANAWA[2]

[1]Department of Radiation Oncology, Aichi Cancer Center Hospital, Aichi, Japan
[2]Department of Radiology, Nagoya University Graduate School of Medicine, Aichi, Japan
*Corresponding author. Department of Radiology, Nagoya University Graduate School of Medicine, 65 Tsurumai-cho, Showa-ku, Nagoya 466-8550, Aichi, Japan; Tel: +81-52-744-2327; Fax: +81-52-744-2335; Email: rie-naka@med.nagoya-u.ac.jp

(Received 6 March 2012; revised 28 May 2012; accepted 13 June 2012)

We analyzed the efficacy of definitive chemoradiotherapy (CRT) for patients with hypopharyngeal cancer (HPC). Subjects comprised 97 patients who were treated with definitive CRT from 1990 to 2006. Sixty-one patients (62.9%) with resectable disease who aimed to preserve the larynx received induction chemotherapy (ICT), whereas 36 patients (37.1%) with resectable disease who refused an operation or who had unresectable disease received primary alternating CRT or concurrent CRT (non-ICT). The median dose to the primary lesion was 66 Gy. The median follow-up time was 77 months. The 5-year rates of overall survival (OS), progression-free survival (PFS), local control (LC), and laryngeal preservation were 68.7%, 57.5%, 79.1%, and 70.3%, respectively. The T-stage was a significant prognostic factor in terms of OS, PFS and LC in both univariate and multivariate analyses. The 5-year rates of PFS were 45.4% for the ICT group and 81.9% for the non-ICT group. The difference between these groups was significant with univariate analysis ($P = 0.006$). Acute toxicity of Grade 3 to 4 was observed in 34 patients (35.1%). Grade 3 dysphagia occurred in 20 patients (20.6%). Twenty-nine (29.8%) of 44 patients with second primary cancer had esophageal cancer. Seventeen of 29 patients had manageable superficial esophageal cancer. The clinical efficacy of definitive CRT for HPC is thought to be promising in terms of not only organ preservation but also disease control. Second primary cancer may have a clinical impact on the outcome for HPC patients, and special care should be taken when screening at follow-up.

Keywords: hypopharyngeal cancer; chemoradiotherapy; survival; laryngeal preservation; local control

INTRODUCTION

Hypopharyngeal cancer (HPC) is usually diagnosed at an advanced stage and treated using multidisciplinary modalities. Chemoradiotherapy (CRT) is currently considered the standard treatment for unresectable head and neck cancer. It is also thought to be a treatment option for patients with resectable locally advanced lesions. Therefore, the number of patients treated with CRT, especially for organ preservation, is increasing. Several types of chemotherapy regimens have been reported to have positive outcomes, and concurrent CRT (CCRT) has become a standard treatment for patients with the aim of preserving the larynx [1, 2]. However, CCRT is reported to be accompanied by markedly increased toxicity compared to radiation alone, and patients who receive CCRT followed by salvage surgery sometimes have serious and intractable complications [3].

Induction chemotherapy (ICT) is often used in clinical practice for patients with advanced HPC and plays a considerable role in organ preservation and reduction of distant metastases [4]. To reduce treatment toxicities and avoid the risk of salvage surgery, we used ICT for patients with resectable tumors with the aim of optimally selecting candidates for larynx preservation.

CCRT regimens with cisplatin (CDDP) and 5-fluorouracil (5-FU) have been used in patients with advanced head and neck cancer. However, severe acute mucositis has been reported with these regimens [2]. For patients treated with

definitive radiotherapy, we have used alternating CRT to reduce acute mucositis during treatment by avoiding concomitant administration of 5-FU without sacrificing the intensity of the chemotherapy.

To evaluate its clinical efficacy, we retrospectively reviewed the clinical results of HPC patients treated with definitive CRT at Aichi Cancer Center Hospital with relatively long follow-up.

MATERIALS AND METHODS

Patient and tumor characteristics

Ninety-seven patients with non-metastatic squamous cell HPC were treated with definitive CRT at Aichi Cancer Center Hospital between 1990 and 2006. The characteristics of the 97 patients are summarized in Table 1. The enrollment criteria were as follows: previously untreated and histologically confirmed squamous cell cancer without distant metastasis. Patients who received radiotherapy alone were excluded from this study. The treatment content of this cohort was as follows: patients with resectable disease and an aim to preserve the larynx received ICT followed by CCRT. Patients who did not want an operation or patients with unresectable disease received alternating CRT or CCRT. Tumors were staged according to the American Joint Committee on Cancer Staging, 5th version [5].

The pre-treatment evaluation consisted of a physical examination, laryngoscopy, biopsy of the primary site, chest radiography, computed tomography (CT) of the cervix and chest, and magnetic resonance imaging (MRI) of the primary site and neck disease. 18-fluorodeoxyglucose-positron emission tomography (18F-FDG PET) or PET/CT was also used after 2001.

Total parenteral nutrition or nasogastric (NG) tube feeding was performed on 39 patients (40%) due to inadequate oral

Table 1. Patient characteristics and treatment contents

Characteristics		All	ICT	non-ICT
Sex	Male	92	59	33
	Female	5	2	3
Age (years)	Median	65	64	66
	Range	36–86	36–80	43–86
Subsite	Postcricoid region	16	7	9
	Pyriform sinus	72	51	21
	Posterior wall	9	3	6
T	1	11	8	3
	2	43	20	23
	3	35	26	9
	4	8	7	1
N	0	33	16	17
	1	16	8	8
	2a	7	6	1
	2b	17	13	4
	2c	17	11	6
	3	7	7	0
Stage	I	5	2	3
	II	19	6	13
	III	22	13	9
	IVA	43	33	10
	IVB	8	7	1
Radiotherapydose (Gy)	Median	66.6	66.6	66.6
	Range	30.6–76.9	30.6–76.9	36–76
IMRT		6	6	0

intake during treatment. In this study a planned gastrostomy was not intended during treatment.

A planned neck dissection was performed in 21 patients (21.6%) who had highly advanced nodal disease (N2b, N2c, or N3) or residual neck disease after CRT. After 2001 the indication of a planned neck dissection was decided by 18F-FDG PET or PET/CT taken within three months after completion of CRT.

Radiotherapy

Ninety-one patients were treated with 3D conformal radiotherapy, and six patients were treated with intensity-modulated radiotherapy (IMRT) using helical tomotherapy. Six patients who were treated with IMRT received ICT. External beam radiotherapy was administered five times a week at a dose of 1.8–2.0 Gy in once-daily fractions using 6-MV photon beams. Treatment planning was made by an X-ray simulator or radiation planning system for 3D conformal radiotherapy.

Patients having conventional radiotherapy were initially treated with opposed lateral fields to the primary and upper neck areas matched to the anterior fields for the lower neck and supraclavicular regions up to 36–40 Gy. The primary lesion and involved neck nodes were further boosted to 66–70 Gy with oblique parallel opposed fields or a dynamic conformal method in order to spare the spinal cord. The gross tumor volume (GTV) was defined as the total volume of the primary lesion and the involved lymph nodes. The GTV was determined by a laryngoscopy, CT, MRI and 18F-FDG PET scan. A positive lymph node was defined as >10 mm in the short axis on CT/MRI or positive 18F-FDG PET findings. The clinical target volume (CTV) was defined as the GTV plus a 10-mm margin to cover microscopic disease. The planning target volume (PTV) was defined as the CTV plus 5-mm margins in every direction. The CTV prophylactic was designed to include the lymph nodes at Levels II–V, the retropharyngeal node and the subclavicular lymph node. The PTV prophylactic was defined as the CTV prophylactic plus 5-mm margins. The initial field included the PTV prophylactic.

Patients receiving IMRT were defined the same as patients receiving conventional radiotherapy. All patients treated with IMRT underwent treatment planning using simultaneous integrated boost methods. A planned delivery dose at D95 was calculated at the PTV/PTV prophylactic for 70 Gy/54 Gy in 35 fractions. Among the patients in this cohort, the median dose to the primary site was 66 Gy (range 30.6–76.9 Gy) and that for the involved lymph node was 63 Gy (range 30–78 Gy).

Chemotherapy

Patients were allocated to receive the ICT or non-ICT protocol (Fig. 1). Patients with resectable disease who aimed to preserve the larynx received ICT, and those who acquired a sufficient response were added to the radiotherapy or CRT protocols. Patients with resectable disease who refused an operation or who had unresectable disease underwent the non-ICT protocol. Of 97 patients, 80 (82%) underwent multi-agent chemotherapy consisting of CDDP and 5-FU (FP) or nedaplatin and 5-FU (FN). Chemotherapy consisted of continuous infusion of 5-FU at a dose of 600 mg/m^2/24 h for five days (Days 1–5). CDDP was given at a dose of 80 mg/m^2/24 h for two days (Days 6 and 7), or nedaplatin was given at a dose of 130 mg/m^2/6 h for one day (Day 6). ICT was used in 61 patients (63%). In the ICT protocol, two courses of FP were administered to 52 patients. Patients who achieved a complete response (CR) with ICT were treated with radiotherapy only, whereas patients who achieved a partial response (PR) received CCRT, which consisted of weekly or triweekly

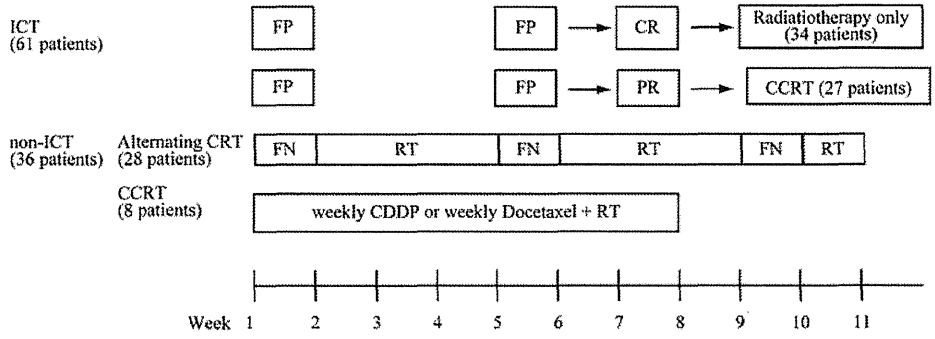

Fig. 1. Treatment scheme of the induction chemotherapy (ICT) group and the non-ICT group. ICT was used in 61 patients (63%). In the ICT protocol, two courses of 5-FU and CDDP (FP) were administered to 52 patients. Patients who achieved a complete response with ICT were treated with radiotherapy only, whereas patients who acquired a partial response received concurrent chemoradiotherapy (CCRT). Non-ICT was used in 36 patients (37%), 28 of whom were administered alternating chemoradiotherapy (CRT) consisting of three cycles of 5-FU and nedaplatin (FN) or 5-FU and CDDP (FP). Another eight patients received CCRT consisting of weekly CDDP or weekly docetaxel.

CDDP. Non-ICT was used in 36 patients (37%), 28 of whom were administered alternating CRT consisting of three cycles of FN or FP. Another eight patients received CCRT consisting of weekly CDDP or weekly docetaxel.

Follow-up

Patients were followed up monthly during the first six months and then every 3–6 months thereafter. Follow-up examinations included a physical examination, laryngoscopy, and a CT or MRI of the neck. 18F-FDG PET or PET/CT was also performed at least annually during follow-ups after 2001. An upper gastrointestinal endoscopy was performed once a year to detect double cancer after the end of CRT. Acute and late toxicity were scored according to the Common Terminology Criteria of Adverse Events, version 3.0 [6].

Statistical analysis

The survival period was calculated from the start of treatment to the date of death or the last follow-up. Progression-free survival (PFS) was defined as the time until an event of disease progression or death of any cause. Local control (LC) was defined as the time until an event of local disease progression or a residual tumor. Laryngeal preservation time was defined as the time until laryngectomy for any reason, except for partial excision. The rates of overall survival (OS), PFS, LC and laryngeal preservation were calculated using the Kaplan-Meier method. The difference between the two groups was tested with the log-rank test. Multivariate analyses were performed using Cox's proportion hazards model. A probability value of <0.05 was defined as significant.

RESULTS

Treatment outcomes

Ninety-four patients (96.9%) completed their scheduled CRT. The median duration of the overall time of ICT-plus-CRT or radiotherapy only was 104 days, and that of alternating CRT was 63 days. At the primary site, 88 patients (90.7%) achieved a CR, 7 (7.2%) had a PR, one (1.0%) had a mild response (MR), and one (1.0%) had progressive disease (PD) after completion of radiotherapy. As for neck disease, 75 patients (79.8%) achieved CR, 17 (17.5%) had PR, one (1.0%) had MR, one (1.0%) had no change, and two (2.0%) had PD. The median follow-up time of this cohort was 77.7 months (range 31.1–175 months). At the last follow-up, 58 (59.8%) of the 97 patients were alive, and 39 (40.2%) had died, of whom 25 (25.7%) patients died from HPC, five patients died from double cancer (two from esophageal cancer, one from lung cancer, one from stomach cancer and one from colon cancer), and nine patients died from other causes (pneumonia in four patients, aspiration asphyxia in one patient and unknown in four patients). Thirty-nine patients (41.2%) were alive without disease and 19 (19.6%) were alive with recurrent disease. The 5-year rates of OS, PFS, LC and laryngeal preservation rates for all patients were 68.7%, 57.5%, 79.1% and 70.3%, respectively. Figure 2 shows the OS curve for all patients and groups. The 5-year rate of OS of groups divided by Stage was 76.9% for Stage I–II and 51.5% for Stage III–IV. The 5-year rate of PFS was 72.3% for Stage I–II and 41.1% for Stage III–IV. The 5-year laryngeal preservation rates of both groups by stage were 85.4% for Stage I–II and 73.2% for Stage III–IV. The LC rate of groups divided by T-stage was 90.0% for T1, 90.1% for T2, 58.5% for T3, and 50.0% for T4 (Fig. 3). In the subgroup analysis, PFS rates at five years were 45.4% in the ICT group and 81.9% in the non-ICT group (Fig. 4); the difference in the PFS rate between these groups was statistically significant ($P = 0.006$).

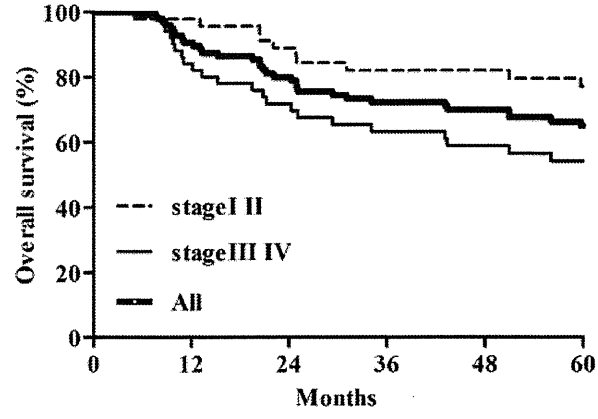

Fig. 2. Overall survival curves of all patients and groups divided by stage.

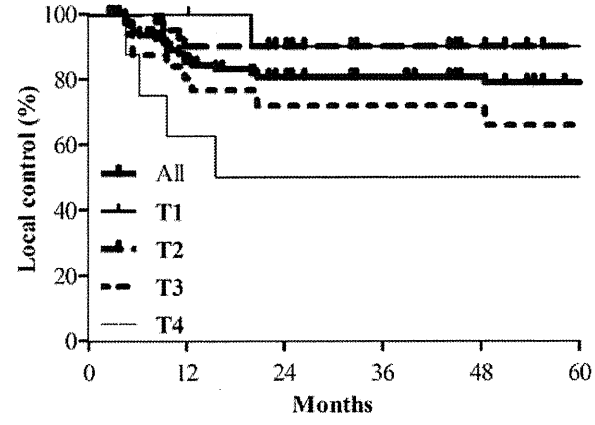

Fig. 3. Local control curves of all patients and groups divided by T-stage.